Richardson Number Profiles over the Continental Shelf

IAN S. F. JONES

RAN Research Laboratory, Darlinghurst, NSW 2010, Australia

(Manuscript received 20 September 1982, in final form 23 May 1983)

ABSTRACT

The seasonal mid-water thermocline over the continental shelf has been examined with the aid of an oceanographic Richardson Number Probe. The overall Richardson number of this stable layer was found to be 0.9 but within the thermocline, regions of low gradient Richardson number were observed. The shape of the conditionally averaged density profile was compared with laboratory experiments and used to aid speculation on the direction of entrainment during this experiment. The low value of the gradient Richardson number in the upper portions of the thermocline supported the interpretation of entrainment from above.

1. Introduction

The water column over the continental shelf is often stratified during the heating season. Atmospheric forcing stirs the upper layer while sea-floor friction due to tidal motions can mix the bottom waters. Within a range of water depths (which appears to encompass a large portion of the outer continental shelf) a strongly stratified thermocline develops between these two mixed layers and persists throughout the summer.

In order to be able to model the transport of momentum through the water column, one must be able to describe the transport of mass and momentum across this stable thermocline. We would like to know the thickness of the thermocline, its maximum gradient, and the rate of entrainment of one homogeneous layer into the other. A useful measure of the dynamic stability of the interface is the Richardson number, i.e., the ratio of the damping of turbulent energy by buoyancy forces to the generation of turbulent energy by velocity shear. Regions of low Richardson number should be turbulent and thus transport mass and momentum in the presence of small mean gradients of these quantities, while regions of high Richardson number should be associated with the strong suppression of turbulence and ineffectual transport of properties down gradients.

In this paper we examine the seasonal thermocline over the continental shelf and determine some statistically stable estimates of the properties of the interface. These statistics are compared with laboratory results in order to speculate on the direction of entrainment and the thickness of sheared interfaces.

2. Apparatus

Profiles of Richardson number were calculated with the aid of an instrument described by Jones and Bruzzone (1981). This Richardson Number Probe (RNP), shown in Fig. 1, measures the velocity difference over a 1.5 m separation and at the same time measures temperature gradient over 1 m. The instrument is changed only slightly from that described by Jones and Bruzzone (1981) by increasing the power to the electromagnetic current meters (to lower the effective electronic noise) and decreasing the current-meter filter time constant to give a -3 dB point of 1 Hz. The electronic noise is 0.5 cm s^{-1} but the fluid mechanical difficulties of flow around the sensors and case probably limit the accuracy to a shear of 10^{-2} s^{-1}. At present our most severe difficulty is in maintaining the zero-shear value to a small fraction of 10^{-2} s^{-1}. The reason for shifts in the zero-shear value is not electronic drift but appears to be connected with the problem of ground-loop currents. The zero-shear value was determined at the site by placing the instrument in a tank of still water that was grounded to the platform from which the measurements were made. Throughout the experiment the same earthing arrangements and cable lengths were maintained. Calibration of the velocity channels of the RNP was carried out before and after the experiment at the University of Sydney towing tank.

The data from the RNP was recorded on the platform with the aid of a 12-bit data logger. This device provided a true average over the sampling period (1 second for this experiment) and wrote the value of each channel, together with the time, on a SEA–DATA cassette tape recorder. Frequent calibration has shown that the data recorder accuracy can be maintained to ± 1 bit, i.e., 0.02% of full scale.

3. Large-scale features of the water column

Measurements were made from the Kingfish B oil recovery platform at a position 148°11′E, 38°36′S in

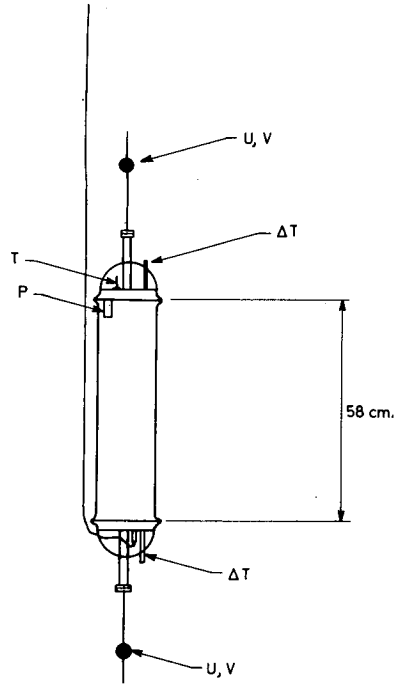

FIG. 1. Gradient Richardson Number Probe. U, V are velocity sensors, T is temperature, ΔT temperature difference and P is pressure.

the eastern portion of Bass Strait. The site is near the shelf break in 78 m of water as shown in Fig. 2. During the summer heating season the water column is often stratified with a well-mixed surface layer separated from a tidally stirred lower layer by a sharp thermocline. The water in Bass Strait is, in general, colder than that of the Tasman Sea and a shelf-break surface front discussed by Godfrey *et al.* (1980) is frequently near the Kingfish B platform.

Internal tides with a semi-diurnal period can cause large movements of the thermocline, and Jones and Padman (1981) found regular waves during periods of strong stratification. These motions, in combination with the shear in the tidal components reported by Jones (1980), complicate the description of shear through the water column. Some preliminary measurements of Richardson number were made in the seasonal thermocline at this site (Jones and Bruzzone, 1981) but our efforts were concentrated on the transient surface thermocline in this previous experiment. When we returned to the site on 5 May 1980, the temperature of the upper mixed layer was 18.2°C and that of the bottom mixed layer was 15.5°C, giving a thermocline strength of 2.7°C. The corresponding change in salinity was 0.13‰ with the upper layer being more saline. During the period of the present measurements the flow was of the order of 30 cm s^{-1} throughout most of the water column and to the west. This fortunately placed the instrument at an upstream corner of the platform legs.

4. Processing of data

The instrument was used to profile across the thermocline, crossing the 17°C isotherm about once per minute. From some 50-odd crossings the data were divided into five periods of 10 minutes, each containing about 10 crossings. The quantities measured during these 10 crossings were simply averaged at each depth and then smoothed with a running filter of the type

$$\bar{P}(z) = \frac{1}{2\Omega}\int_{z-\Omega}^{z+\Omega} P(z)dz, \qquad (1)$$

where z is defined positive in the upward direction.

The variables measured, $P(z)$, were spatial averages of the type

$$P(z) = \frac{1}{\delta z}\int_{z}^{z+\delta z} \frac{\partial P}{\partial z}\, dz,$$

where δz was 83 cm for temperature difference δT and 145 cm for velocity difference δU, i.e., the sensor separations.

By adjusting the averaging distance in Eq. (1) both sensors have the same effective vertical averaging distance (of an equivalent box-car filter) of 145 cm. The spatial filter is shown as an insert in Fig. 3.

All the averaged profiles of temperature gradient had the same visual appearance with a narrow region at the bottom of the density interface where the gradient rose rapidly from its value near zero in the bottom mixed layer to around 0.5 × 10^{-2} °C cm^{-1}. As

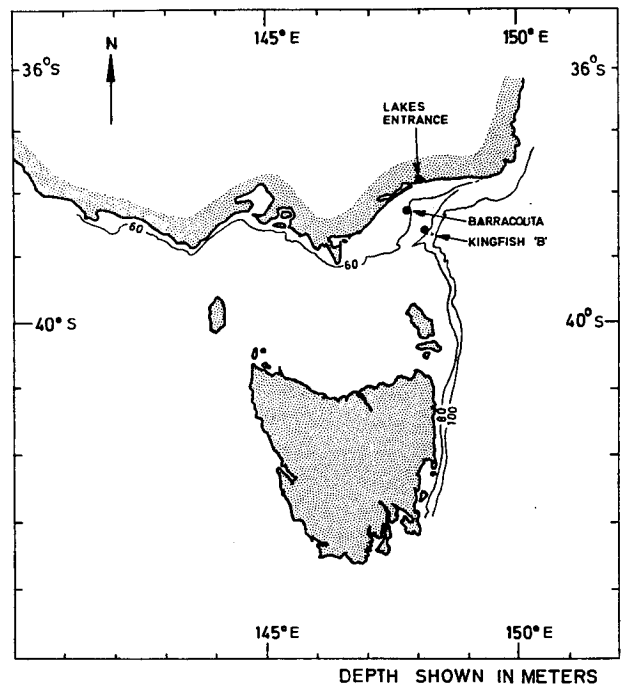

FIG. 2. Location of the Kingfish B platform from which measurements were made.

Fig. 3 shows, the temperature gradient decreases slowly to a low value in the upper mixed layer. In contrast, the velocity gradients were more variable, but in the north-south direction there appeared to be a significant gradient associated with the density gradient. Tidal forcing produces a counterclockwise rotary current at this site with the upper current lagging the lower current in the manner illustrated in Fig. 4 of Jones (1980). For the profiles in Fig. 3 the current was rotating from NW to SW and the lagging upper current induced much of the shear over the middle portions of the water column. Those velocity profiles that extended some distance from the interface showed that the shear zone was much thicker than the zone of significant temperature gradient.

The generation of a stable statistic in a variable geophysical flow is difficult. The thermocline is deepening during the 50-minute measurement period, in part because of the internal tidal motion discussed by Jones and Padman (1983). From the Richardson Number Probe yoyo dips, the depth of the 17°C isotherm is plotted in Fig. 4, as well as the maximum temperature gradient, i.e.,

$$\frac{1}{\delta z}\int_{z}^{z+\delta z}\frac{\delta T}{\delta z}\,dz, \quad \delta z = 83 \text{ cm},$$

of each interface crossing. Obviously an average at constant depth smears out the temperature gradient and so averages were computed relative to the 15.6°C-isotherm position of each 10-minute sample. Using the five profiles in Fig. 3 the conditional averages (at depth relative to the 15.6°C isotherm) are shown in Fig. 5. The width of the 50-minute average of temperature gradient was 3.7 m between points that were e^{-1} of the maximum average temperature gradient. This interface, which is of comparable thickness to the transient thermocline described by Jones and Bruzzone (1981), is much thinner than many interfaces found at the bottom of the surface mixed layer during JASIN 78. The north and south velocity gradients were similarly averaged and the vector sum of the two conditionally averaged gradients used to compute

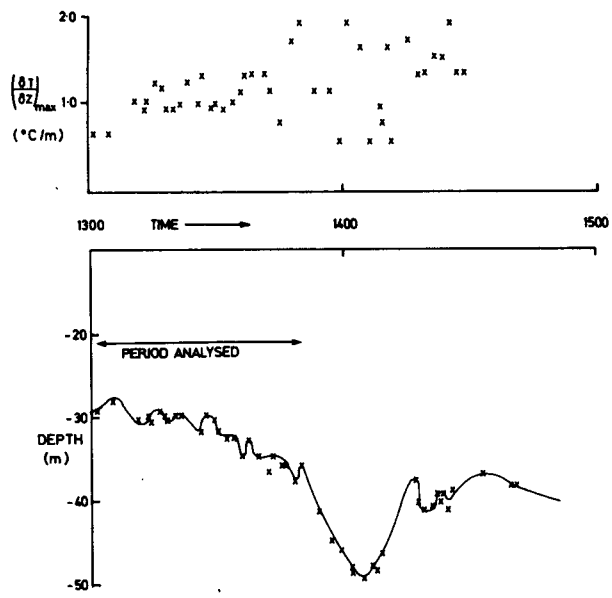

FIG. 4. Depth of the 17°C isotherm together with the maximum temperature gradient (averaged over 0.8 m).

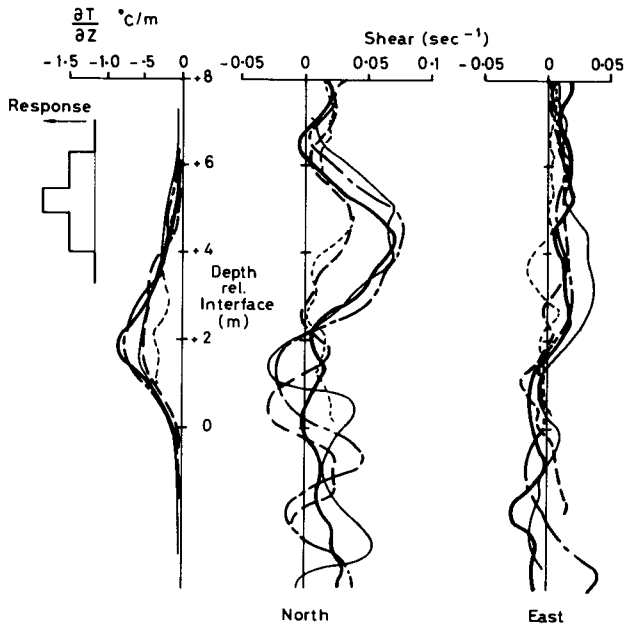

FIG. 3. Temperature gradient and velocity gradient measurements on day 65, 1980. Each trace is a 10-minute average. The spatial filter used is shown in the upper left corner.

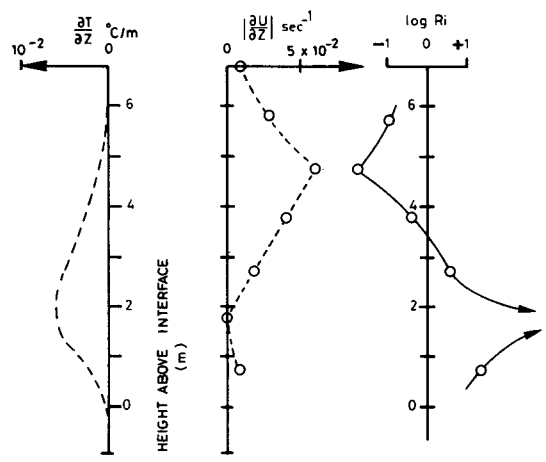

FIG. 5. Ensemble-averaged temperature gradient and velocity shear together with the Richardson number calculated from these curves. Day 65, 1980.

$$\left|\frac{\partial U}{\partial z}\right|^2 = \left(\frac{\partial \overline{U}_N}{\partial z}\right)^2 + \left(\frac{\partial \overline{U}_E}{\partial z}\right)^2.$$

The velocity gradient was most pronounced a distance above the sharpest temperature gradient and maintained this position relative to the 15.6°C isotherm despite considerable deepening of the interface during the 50-minute averaging period.

We must conclude that the shear and temperature gradient in Fig. 5 are associated in some sense. The maximum temperature gradient of each crossing (shown in Fig. 4) becomes more variable throughout the experiment but shows no trend during the period. It follows the 15.6°C isotherm as it deepens and the profiles relative to this isotherm can be seen in Fig. 3. The region of extended shear (in the north direction) also deepens in conjunction with the isotherms. Thus it appears that the position of the shear that is imposed by the tidal flow and the temperature interface between the upper and lower layer of the water follow each other. If this were not the case, averaging relative to the 15.6°C isotherm would be expected to smear out the velocity gradient. We might have expected the highest shear to occur at the same depth as the maximum temperature gradient but this was not the case. The average shear was largest some 3 m above the maximum temperature gradient.

From the width, the temperature difference between the upper and lower layers (ΔT) and the velocity difference (ΔU) determined from integration of Fig. 5, we can calculate an interface Richardson number. The buoyancy jump results from both the temperature and salinity difference, but if we assume a temperature–salinity relation, the buoyancy jump can be approximated by $g\alpha\Delta T$. We have used $\alpha = 2 \times 10^{-4}$ (°C)$^{-1}$ for the present situation. Relevant bulk parameters of the interface are given in Table 1. We find that the interface is stable on overall measures with a bulk Richardson number of 0.9. Since this thermocline persists throughout most of the summer we would not expect to find the low Richardson number observed by Jones and Bruzzone (1981) for the transient thermocline.

TABLE 1. Details of thermocline for 1300–1400 Day 65, 1980.

Water depth	76 m
Mean depth of 17°C isotherm, D	32 m
Width of thermocline e^{-1}, L_ρ	3.7 m
Average temperature difference ΔT	2.7°C
Average velocity difference ΔU	14.3 cm s^{-1}
Bulk Richardson number, $\frac{g\alpha\Delta T L_\rho}{\Delta U^2}$	0.9
Inverse Froude number, $g\alpha\frac{\Delta T D}{\Delta U^2}$	8.5
Wind speed	5 m s^{-1}
Wind stress, τ	0.3 dyn cm^{-2}
Significant wave height	0.9 m
Representative current speed	30 cm s^{-1}
Inverse Froude number, $\frac{g\alpha\Delta T D\rho}{\tau}$	5.8×10^3
Buoyancy time scale, $\frac{\Delta U}{g\alpha\Delta T}$	30 s

5. Local Richardson number

For the quantities averaged over 50 min we can calculate the local Richardson number,

$$\mathrm{Ri}(z) = \frac{g\alpha\overline{\partial T/\partial z}}{(\partial U/\partial z)^2},$$

where the overbar implies a temporal and spatial average. We have assumed that the density gradient, normalized by the mean density, is dominated by the temperature gradient. The logarithm to the base of 10 of Ri(z) is presented in Fig. 5.

One sees within the thermocline minimum local Richardson numbers of about 0.05 despite the bulk Richardson number of the interface being 0.9. The differing shapes of the shear and the temperature profiles are responsible for the large differences between the two measures of stability. Also there is a region of high local stability and presumably it is this portion of the interface that inhibits mixing.

If we examine shorter time scales we see that both the temperature (density) and the shear fluctuate about their 50-min mean values. These fluctuations induce variations in the gradient Richardson number. Jones and Bruzzone (1981) showed such fluctuations in the seasonal thermocline when one-second averages were used.

A suitable averaging time to use in calculating Richardson number is difficult to determine. Both the overturn time of an eddy, calculated with thickness of the interface (L_ρ), i.e., $L_\rho/\Delta u \approx 24$ s, and the buoyancy time scale (see Table 1) of 30 s appear to be short compared with the time scale of shear fluctuations that we observed. One would like an averaging time that is longer than that required for significant turbulent energy to be generated. This is in turn a function of the Richardson number since low Richardson number implies that little turbulent energy is lost to buoyancy damping while high Richardson number implies that most of the shear-generated turbulence is lost immediately to buoyancy damping. To form a time scale, θ, in a zero Richardson number flow, indicative of the rate of change of turbulent energy, one can equate the rate of change of turbulent energy to the rate of generation, G, i.e.,

$$\frac{\text{turbulent energy}}{\theta} = G.$$

Thus it follows that since the generation is of the order of the product of turbulent energy and the shear, θ is proportional to $L_\rho/\Delta U$.

When the buoyancy term B is also included in the energy balance, i.e.,

$$\frac{\text{turbulent energy}}{\theta} = G - B = G(1 - \text{Ri}),$$

the time scale becomes

$$\theta = \frac{L_\rho}{(1 - \text{Ri})\Delta U}.$$

In the present case θ is 5 min, and we have somewhat arbitrarily averaged over 10 minutes, twice this period.

When we use the 10-min averages of Fig. 3 to calculate the gradient Richardson number, we obtain the values given in Table 2. At 1.7 m above the 15.6°C isotherm (z^* = 1.7 m) the 50-min average Richardson number (Ri = 180) indicates a very stable situation but the Richardson number calculated from 10-min averages is in the range 1 to 10. Thus despite the high stability over long times, on time scales needed for the build-up of turbulent energy the gradient Richardson number drops to order unity for some period. The fluctuations in the shear are responsible for this difference of Richardson number with time and the low value of long-term shear leads to the high value of the 50-min average Richardson number.

If we look at the Richardson number near the point of maximum shear (z^* = 4.7 m) the fluctuations in the 10-min average Richardson number are small. The variations in shear, as one can see from Fig. 3, are about the same as those at z^* = 1.7 m but since they are about a large mean, the Richardson number is only weakly affected. At this position the Richardson number is below 0.25 for each 10-min period and we expect mixing of fluid away from the more stable layer below.

6. Interface thickness

When a density interface is subjected to shear, the interface broadens until some Richardson number becomes too large to support turbulent mixing. In a situation where there is a turbulent layer on one side of the interface, it reaches a steady thickness but continues to entrain. Jones and Mulhearn (1983) describe such an experiment in an annular tank where both external turbulence and shear were found to influence the rate of entrainment. This same apparatus was used to study the profile that developed between two constant density layers. The rotating screen induced a velocity difference ΔU across the interface whose profile was measured using a single point conductivity probe. While the rotating screen applying the surface stress to the tank was coarser than that described by Jones and Mulhearn, this change appeared to be of little significance.

TABLE 2. Richardson numbers from 10 minute averages.

Time (−10 h GMT)	z^* = 1.7 m	z^* = 4.7 m
1300–1310	1.6	0.09
1310–1320	3.7	0.07
1230–1330	9.6	0.06
1330–1340	2.6	0.06
1340–1350	4.4	0.18
1300–1350	180.0	0.06

z^* distance above interface

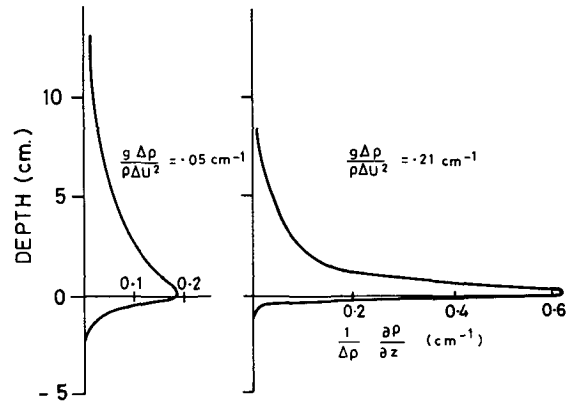

FIG. 6. Density gradients measured in an annular tank. Data averaged at constant depth.

From averages of density at constant depth, the density gradient was determined and plotted in Fig. 6 relative to the depth of maximum gradient. Considerable smoothing of the profile resulted from this process since the interface deepened about 0.1 of its thickness during the measurement. It is immediately evident that these profiles are asymmetric about the maximum gradient with the gradient decreasing more rapidly on the side away from the turbulent layer.

From the density jump and the velocity jump across these interfaces one can construct a buoyancy length

$$L_B = \frac{\rho(\Delta U)^2}{g\Delta\rho}.$$

At smaller buoyancy lengths (very stable) the thickness of the interface becomes comparable with the oscillations of the interface and averaging at a fixed depth gives difficult-to-interpret results.

However, for the buoyancy lengths in these two tank experiments, the observed interface oscillations appeared to be considerably less than the width of the profiles and so it seems reasonable to compare the results in Fig. 6 with the conditional averages, dependent on the distance from an isotherm, used in Fig. 5. When one considers the oceanic profile about the maximum gradient of temperature (z^* = 1.8 m) the gradient changes more slowly above z^* = 1.8 m than below z^* = 1.8 m. This is similar to the laboratory result.

The interface thickness L_ρ has been determined from these two profiles and is plotted in Fig. 7 as a function of buoyancy length. The present Bass Strait interface is much thicker than the laboratory interfaces but is narrower than the transient thermocline examined by Jones and Bruzzone (1981). Also shown in Fig. 7 is the transient halocline measured by Price (1979) that followed rain over the Florida continental shelf. In this case we have approximated L_ρ by $0.8d$ where d is his halocline width.

One sees the trend of increasing interface thickness with increasing buoyancy length. It follows that it will be difficult to establish a mildly stable shear layer in a laboratory tank without the shear layer interacting with the top and bottom of the tank.

If the interface thickness were always greater than a certain fraction of the buoyancy length, then a critical bulk Richardson number would exist. This would lead to an expression

$$L_\rho > R_c L_B.$$

One can explain such an inequality by speculating that if L_ρ drops below the critical value the interface thickens because of internally generated turbulence. However, if the buoyancy length decreases, on account of reduced shear for example, the thickness L_ρ remains greater than $R_c L_B$. External turbulence may well scour the outer edges of the interface, gradually reducing L_ρ. Since in laboratory experiments the rate of entrainment depends upon both buoyancy length and external turbulence, it is not unreasonable to expect the interface thickness also to be a function of such external variables. We have as yet too little data to resolve this question.

Pollard *et al.* (1973) made popular the suggestion that during entrainment a Froude number,

$$\frac{\rho(\Delta U)^2}{g\Delta\rho D}$$

should be constant, where D is the distance from the surface applying a stress to the interface. For the data in Fig. 7 the range of Froude number is large with inverse Froude numbers of 2 and 8 for the annular tank, 8.5 for the present experiment, 0.6 for Price's (1979) data, and 0.3 for the data of Jones and Bruzzone (1981). One could argue that the relationship between the surface stress and velocity jump ΔU was complex in all cases except the two transient thermoclines, and indeed this is so, with much momentum lost to the side walls in the annular tank and much of the shear induced by internal tides in the present oceanic case. Thus, the distance from the surface applying the stress to the interface may not be the dominant length scale. This observation, however, merely points out that Froude number does not provide a closure by itself of the problem of sheared stable interfaces. The bulk Richardson number appears to be more nearly constant than the Froude number.

7. Entrainment

It is not possible in the ocean to deduce the direction of entrainment from the short-term movement of the interface because of the influence of internal waves that can move the interface much faster than one layer can entrain the other across a stable interface. However, the temperature gradient in Fig. 5,

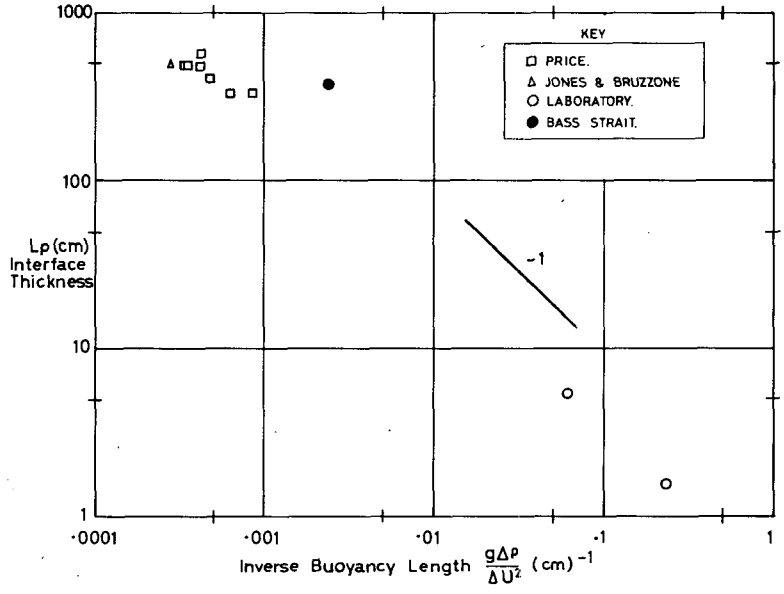

FIG. 7. The density length scale as a function of the buoyancy length.

with steeper gradients at the bottom of the thermocline, may be characteristic of entrainment by reasonably stable sheared interfaces. It is similar to the slope of the profiles in the laboratory experiments that entrained fluid from below.

We imagine that, in both the laboratory experiment and the present oceanic situation, the shear at the interface induces mixing, and this mixed fluid is swept away by the turbulence of the upper layer. The lower density gradients of the broad portion of the thermocline about the density gradient maximum require higher diffusivities to transport the same flux of density as the lower portion of the thermocline. The Richardson number profiles in our present situation are consistent with this model, with lower Richardson numbers in the upper turbulent portions of the interface where we speculate that the diffusivity is high.

In the laboratory situation there clearly was no turbulent motion below the interface while over the continental shelf we must assume for the period studied that the effective turbulence is less in the layer below the interface than in the layer above.

We can contrast this profile through the seasonal thermocline with that observed in 1978 by Jones and Bruzzone (1981), in a near-surface transient thermocline that was between the seasonal thermocline and the surface. The transient thermocline exhibited little asymmetry in the temperature gradient profile and the bulk Richardson number of 0.16 was much less than in the present case. This thermocline presumably did not persist for long. We may speculate, from observing these density profiles, that the asymmetric nature of the interface is a function of the stability of the interface. Interfaces of low stability are symmetric about their mid-point (near-neutral density shear layers have a temperature profile that is close to an error function (see Fiedler, 1974), while strongly stable interfaces may take on an asymmetry indicative of the directional nature of the (small) entrainment. More examples are needed to test this speculation.

8. Conclusions

Measurements have been presented of the detailed structure of an interface between a wind-mixed layer of warm water and a cold layer mixed by bottom friction. This thermocline was found to have a bulk Richardson number near unity but within the interface (on time scales representative of the growth of turbulence within a shear layer of this thickness) regions of much higher stability were observed in the lower portions of the thermocline. The asymmetric nature of the density profile observed in this case is similar to that observed in laboratory experiments and may be an indicator of the direction of entrainment. Entrainment is to the more turbulent layer from the less turbulent. The extended region of density gradients and the lower Richardson number on the upper side of the thermocline point to this being the more turbulent region and suggest that entrainment in the present situation is upward.

The thickness of the sheared stable interfaces examined did not drop below a certain fraction of the buoyancy length. Large buoyancy lengths (decreased stability) were associated with thick interfaces. Active entraining interfaces, as well as being asymmetric, are in equilibrium between scouring of external turbulence, which decreases interface thickness, and turbulence within the sheared regions, which attempts to thicken the interface.

REFERENCES

Fiedler, H. E., 1974: Transport of heat across a plane turbulent mixing layer. *Advances in Geophysics,* Vol. 18, Academic Press, 93.

Godfrey, J. S., I. S. F. Jones, J. G. H. Maxwell and B. D. Scott, 1980: On the winter cascade from Bass Strait into the Tasman Sea. *Aust. J. Mar. Freshwater Res.*, **31,** 275–286.

Jones, I. S. F., 1980: Tidal and wind-driven currents in Bass Strait. *Aust. J. Mar. Freshwater Res.*, **31,** 109–117.

——, and F. Bruzzone, 1981: An oceanographic Richardson Number Probe. *Deep-Sea Res.*, **28A,** 507–519.

——, and L. Padman, 1981: Semidiurnal internal tides in eastern Bass Strait. *Aust. J. Mar. Freshwater Res.* **34,** 159–171.

——, and P. J. Mulhearn, 1983: The influence of external turbulence on sheared interfaces. *Geophys. Astrophys. Fluid Dyn.* **24,** 49–62.

Pollard, R. T., P. B. Rhines and R. O. R. Y. Thompson, 1973: The deepening of the wind-mixed layer. *Geophys. Fluid Dyn.*, **3,** 381.

Price, J. F., 1979: Observations of a rain-formed mixed layer. *J. Phys. Oceanogr.*, **9,** 643.